

Study of Higgs plus single top production using events with a same sign dimuon at the Large Hadron Collider

L.F. Hiram Ernesto Damián

Director:

José Feliciano Benítez Rubio

Maestría en Ciencias (Física)

Departamento de Investigacion en Física

Universidad de Sonora

November 15th 2019



1 Introduction

- Standard Model
- Higgs mechanism
- Higgs production mechanisms and decays

2 LHC and CMS

- LHC
- CMS detector

3 Event selection and reconstruction

- Topology of tH
- Main backgrounds
- Event selection
- BDT
- Previous results
- Systematic uncertainties

4 Statistical analysis

- Likelihood model
- Results

5 Results



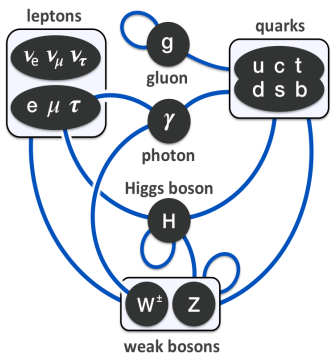
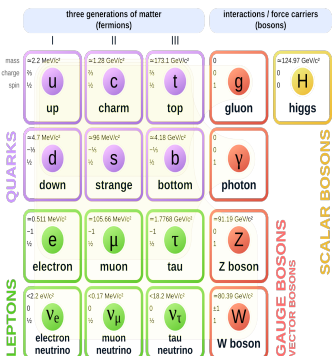
Motivation for single top Higgs (tH)

- Coupling measurement is essential to establish the nature of the Higgs
- The exploration of Higgs production on the tH channel is subject relatively new. Measurements of CMS and ATLAS are compatible with SM predictions.
- The tH study explores the relative sign of top-Higgs and W-Higgs couplings.
Small deviations from SM predictions could be associated with physics beyond the standard model (BSM) such as String Theory and Supersymmetry.



Standard Model

Standard Model of Elementary Particles



Particles Properties

Table of particles in SM

Particle	Mass (MeV/ c^2)	Charge	spin	Lifetime (s)	Distance in lifetime (meters)
Up (u)	2.2	$\frac{2}{3}$	$\frac{1}{2}$	stable	-
Charm (c)	1280	$\frac{2}{3}$	$\frac{1}{2}$	1.1×10^{-12}	5.21×10^{-3}
Top (t)	173100	$\frac{2}{3}$	$\frac{1}{2}$	5×10^{-25}	2.37×10^{-15}
Down (d)	4.6	$-\frac{1}{3}$	$\frac{1}{2}$	Stable	-
Strange (s)	96	$-\frac{1}{3}$	$\frac{1}{2}$	1.24×10^{-8}	58.7
Bottom (b)	4180	$-\frac{1}{3}$	$\frac{1}{2}$	1.3×10^{-12}	6.16×10^{-3}
W	80379	± 1	1	3×10^{-25}	1.42×10^{-15}
Z	91187.6	0	1	3×10^{-25}	1.42×10^{-15}
Photon (γ)	0	0	1	Stable	-
Gluon (g)	0	0	1	Stable	-
Higgs (H)	125.18	0	0	1.56×10^{-22}	7.39×10^{-13}
Electron (e)	0.511	-1	$\frac{1}{2}$	Stable	-
Muon (μ)	105.7	-1	$\frac{1}{2}$	2.2×10^{-6}	10419.85
τ	1776.86	-1	$\frac{1}{2}$	2.9×10^{-13}	1.37×10^{-3}
$\nu_e \nu_\mu \nu_\tau$	0	0	$\frac{1}{2}$	Stable	-



Electroweak SM Lagrangian

Higgs lagrangian

$$\mathcal{L}_{\text{Higgs}} = (D_\mu \Phi)^\dagger (D^\mu \Phi) - V(\Phi^\dagger \Phi) \quad (1)$$

with

- $D_\mu \Phi = \left(\partial_\mu + (ig/2)\sigma^i W_\mu^i - i\frac{1}{2}g' B_\mu \right) \Phi$
- $V(\Phi^\dagger \Phi) = -\mu^2 \Phi^\dagger \Phi + \frac{1}{2}\lambda(\Phi^\dagger \Phi)^2, \quad \mu^2 > 0$
- $\Phi = \begin{pmatrix} \phi^+ \\ \phi^0 \end{pmatrix}$ is a SU(2) doublet.
- σ^i are the Pauli matrices.
- Φ is higgs field which is a complex scalar field. Φ
- λ and μ^2 are Higgs potential parameters



SM Lagrangian

Yukawa lagrangian

$$\mathcal{L}_{\text{yukawa}} = \sum_{m,n}^3 \Gamma_{mn}^u \bar{q}_{m,L} \tilde{\Phi} u_{n,R} \quad (2)$$

where h.c is hermitian conjugate. m and n are flavors of quarks and leptons.

The matrices Γ_{mn} describe the so called Yukawa couplings between higgs doublet ϕ and the fermions.

Choosing

$$\Phi = -\frac{1}{2} \begin{pmatrix} 0 \\ v + h \end{pmatrix}$$

By using 3 it on $\mathcal{L}_{\text{yukawa}}$, it is obtained for u quark

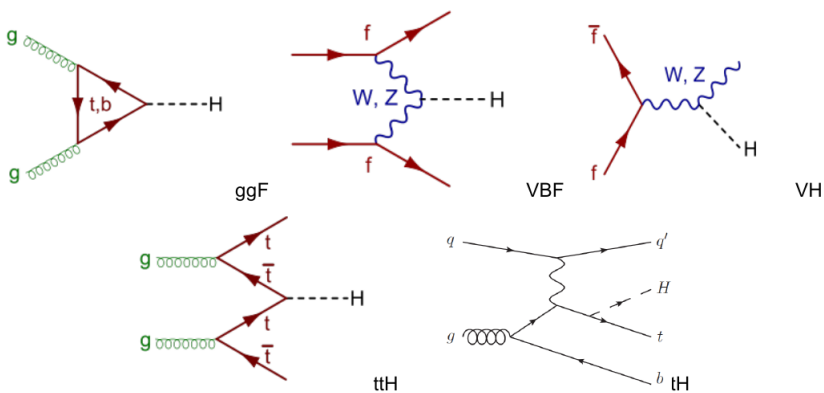
$$\frac{\Gamma_{uu}^u v}{\sqrt{2}} (\bar{u}_L u_R + \bar{u}_R u_L)$$

from which the masses for the fermions shown to be proportional to the Yukawa couplings

$$m_u = -\frac{\Gamma_{uu}^u v}{\sqrt{2}}$$

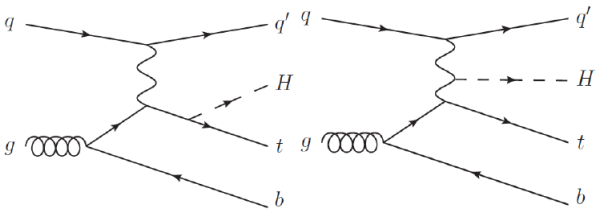


Higgs production mechanisms



Different Higgs production mechanism, from the most likely to least likely

tH production mechanisms



tH mechanism. Higgs radiated from a top quark (left). Higgs radiated from a W boson (right)

tH production mechanisms

- In a proton proton collision, the production cross section of the single top plus Higgs boson process is driven by a destructive interference of two main diagrams, where the Higgs couples to either the W boson or the top quark.
- A second process, where the Higgs and top quark are accompanied by a W boson (tHW) has similar behavior, albeit with a weaker interference pattern.
- However, in the presence of new physics, there may be relative opposite signs between the tH and WH couplings which lead to constructive interference and enhance the cross sections by an order of magnitude or more.



Cross section

- Cross section describes the likelihood of two particles interacting under certain conditions[1][8]
- Experimentally

$$d\sigma = \frac{\text{number of particles scattered into solid angle } \Delta\Omega}{(\text{number of particles incident})(\text{scattering centers/area})} \quad (3)$$

- Cross sections are expressed in barns , where $1 \text{ barn} = 10^{-34} \text{ cm}^{-2}$
- The reaction rate N_R is determined by the total cross section σ and the incident flux L .
 L is called luminosity and it is measured in $\text{cm}^{-1}\text{s}^{-1}$.[8]

$$N_R = \sigma L$$

(4)



Higgs production Cross section

Higgs boson production cross sections in pp collisions for $\sqrt{s} = 13\text{TeV}$ (in pico barn). Integrated luminosity of 35.9 fb^{-1} for Run 2¹

Production mechanism	σ (picobarns pb)	Number of events
ggF	48.93	1756587
VBF	3.78	135702
WH	1.35	48465
ZH	0.88	31592
t <bar>t>H</bar>	0.50	18255
tH (only)	0.015	560.39

¹Data taken from The cern collaborarion "Higgs Physics the HL-LHC and HE-LHC" 2019,
CERN-LPCC-2018-04



Branching ratio

In particle physics, the branching ratio for a decay process is the ratio of the number of particles which decay via a specific decay mode with respect to the total number of particles which decay via all decay modes.
².

$$\text{BR} = \frac{\Gamma_i}{\sum_i \Gamma_i} \quad (5)$$

Where $\Gamma = \sum_i \Gamma_i$ is the total decay width (sum of all partial widths) of the particle and is related to lifetime of the particle: $\Gamma = 1/\tau$. Since the dimension of Γ is the inverse of time, in our system of natural units, it is measured in inverse seconds.⁰

⁰Cleaves H.J. (2011) Branching Ratio. In: Gargaud M. et al. (eds) Encyclopedia of Astrobiology. Springer, Berlin, Heidelberg

Higgs Branching ratios per channel

SM Higgs boson branching ratios for $M_H = 125$ GeV

Higgs decay	Branching ratio (BR)
$H \rightarrow b\bar{b}$	50.82%
$H \rightarrow W^+W^-$	21.5%
$H \rightarrow \tau^+\tau^-$	6.27%
$H \rightarrow ZZ$	2.61%
$H \rightarrow \gamma\gamma$	0.227%
$H \rightarrow Z\gamma$	0.153%
$H \rightarrow \mu^+\mu^-$	0.0217%

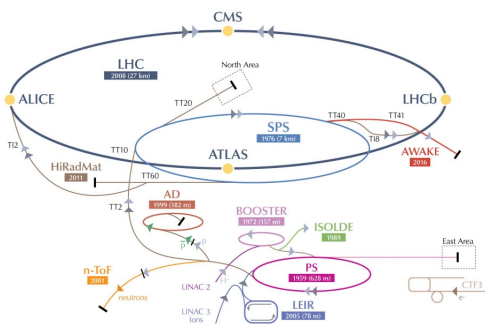
$\mu\mu$ same sign decay rate

Table of decay chains for tH . Expected number of tH final states events for 35.9 fb^{-1} . l represents μ^\pm, e^-, τ^\pm .

Decay chain	BR	Events
$tH \rightarrow W^+ b W^+ W^- \rightarrow \mu^+ \nu_\mu b \mu^+ \nu_\mu q \bar{q}'$	2.096×10^{-3}	1.173
$tH \rightarrow W^+ b W^+ W^- \rightarrow \mu^+ \nu_\mu b \mu^+ \nu_\mu l^- \bar{\nu}_l$	3.37×10^{-4}	0.899
$tH \rightarrow W^+ b \tau^+ \tau^- \rightarrow \mu^+ \nu_\mu b \mu^+ \nu_\mu \nu_\tau l^- \bar{\nu}_l \nu_\tau$	3.637×10^{-4}	0.203
$tH \rightarrow W^+ b W^+ W^- \rightarrow \tau^+ \bar{\nu}_\tau b \mu^+ \nu_\mu q \bar{q} \rightarrow \mu^+ \nu_\mu \bar{\nu}_\tau \bar{\nu}_\tau b \mu^+ \nu_\mu q \bar{q}$	1.890×10^{-4}	0.105
$tH \rightarrow W^+ b \tau^+ \tau^- \rightarrow \mu^+ \nu_\mu b \nu_\tau \mu^+ \nu_\mu \bar{\nu}_\tau q \bar{q}$	1.681×10^{-4}	0.094
$tH \rightarrow W^+ b W^+ W^- \rightarrow \tau^+ \bar{\nu}_\tau b \mu^+ \nu_\mu l^- \bar{\nu}_l \rightarrow \mu^+ \nu_\mu \bar{\nu}_\tau \bar{\nu}_\tau b \mu^+ \nu_\mu l^- \bar{\nu}_l$	3.045×10^{-5}	0.017
$tH \rightarrow W^+ b ZZ \rightarrow q \bar{q} b ZZ \rightarrow q \bar{q} b \mu^+ \mu^- \mu^+ \mu^-$	1.966×10^{-5}	0.011
$tH \rightarrow W^+ b \tau^+ \tau^- \rightarrow \tau^+ \bar{\nu}_\tau b \mu^+ \nu_\mu \bar{\nu}_\tau q \bar{q}' \nu_\tau \rightarrow \mu^+ \nu_\mu \bar{\nu}_\tau \bar{\nu}_\tau b \mu^+ \nu_\mu \bar{\nu}_\tau q \bar{q}' \nu_\tau$	1.549×10^{-5}	0.008

LHC

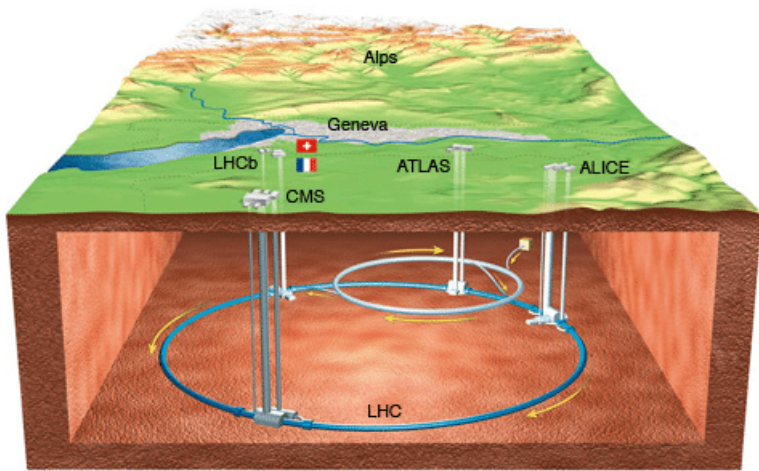
CERN's Accelerator Complex



LHC complex



LHC



Underground view of LHC complex

LHC parameters

Characteristics of LHC

Quantity	Number
Circumference	26 659 m
Number of magnets	9593
Nominal energy, protons	6.5 TeV
Nominal energy, protons collisions	13 TeV
Number of collisions per second	1 billion
No. of bunches per proton beam	2808

Accelerator operation energies

Accelerator	Energy
Linac 2	50 MeV
PS Booster	1.4 GeV
Proton Scyncroton (PS)	25 GeV
SPS	450 GeV
LHC	6.5 TeV

CMS detector

CMS DETECTOR

Total weight : 14,000 tonnes
Overall diameter : 15.0 m
Overall length : 28.7 m
Magnetic field : 3.8 T

STEEL RETURN YOKE
12,500 tonnes

SILICON TRACKERS
Pixel (100x150 μm) ~16 m^2 ~66M channels
Microstrips (80x180 μm) ~200 m^2 ~9.6M channels

SUPERCONDUCTING SOLENOID
Niobium titanium coil carrying ~18,000A

MUON CHAMBERS
Barrel: 250 Drift Tube, 480 Resistive Plate Chambers
Endcaps: 468 Cathode Strip, 432 Resistive Plate Chambers

PRESHOWER
Silicon strips ~16 m^2 ~137,000 channels

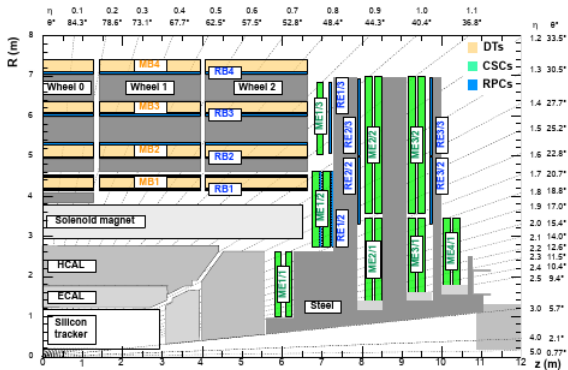
FORWARD CALORIMETER
Steel + Quartz fibres ~2,000 Channels

CRYSTAL
ELECTROMAGNETIC
CALORIMETER (ECAL)
~76,000 scintillating PbWO₄ crystals

HADRON CALORIMETER (HCAL)
Brass + Plastic scintillators ~7,000 channels

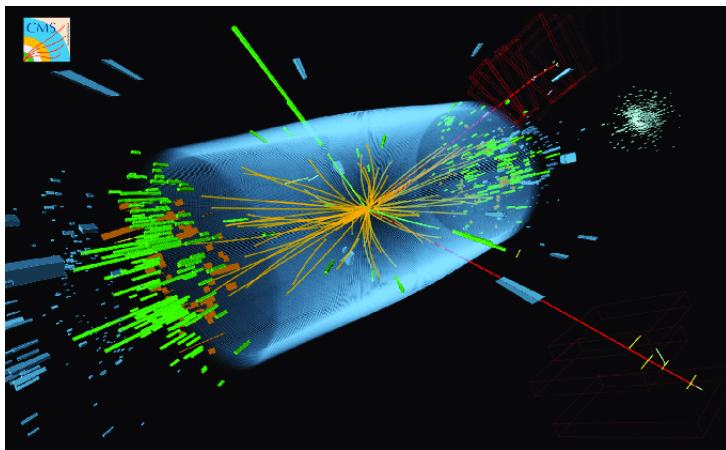
Compact muon solenoid

CMS detector



Slide view of the CMS in terms of pseudorapidity $\eta = -\ln [\tan (\frac{\theta}{2})]$

CMS detector

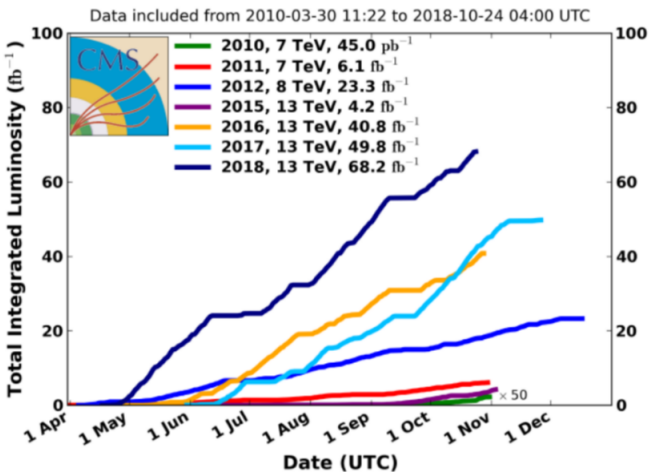


A typical CMS event display of the Higgs boson decaying to four leptons with 2 muons (in red) and 2 electrons (in green) as final state signatures



CMS integrated luminosity

CMS Integrated Luminosity, pp

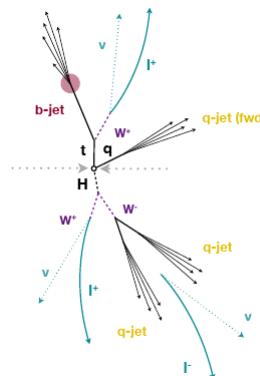


Integrated luminosity for CMS experiment

Topology of events tH

The characteristics of the signal tH :

- $t \rightarrow W^+ b \rightarrow l^+ \nu_\mu b$
- $H \rightarrow W^+ W^-$
 - $W \rightarrow l^\pm \nu$, where l can be μ^\pm, e^\pm, τ^\pm
 - $W \rightarrow q\bar{q}$
 - W bosons decay leptonically resulting in a signature of two same-sign leptons
- a light-flavor quark
- A b-jet



Main backgrounds

Main backgrounds and their same sign $\mu\mu$ decay process

Background	Decay process
$t\bar{t}W$	$t\bar{t}W \rightarrow W^+ b W^- \bar{b} \mu^+ \nu_\mu \rightarrow \mu^+ \nu_\mu b \mu^- \bar{\nu}_\mu \bar{b} \mu^+ \nu_\mu$
$t\bar{t}Z$	$t\bar{t}Z \rightarrow W^+ b W^- \bar{b} \mu^+ \mu^- \rightarrow \mu^+ \nu_\mu b \mu^- \bar{\nu}_\mu \bar{b} \mu^+ \mu^-$
$W^+ Z$	$W^+ Z \rightarrow \mu^+ \nu_\mu \mu^+ \mu^-$
$W^\pm W^\mp$	$W^+ W^+ \rightarrow \mu^+ \nu_\mu \mu^+ \nu_\mu$
tZq	$tZq \rightarrow W^+ b \mu^+ \mu^- q \rightarrow \mu^+ \nu_\mu b \mu^+ \mu^- q$
$t\bar{t}t\bar{t}$	$t\bar{t}t\bar{t} \rightarrow W^+ b W^- \bar{b} W^+ b W^- \bar{b} \rightarrow \mu^+ \nu_\mu b \mu^- \bar{\nu}_\mu \bar{b} \mu^+ \nu_\mu b \mu^- \bar{\nu}_\mu \bar{b}$
$W^+ W^- Z$	$W^+ W^- Z \rightarrow \mu^+ \nu_\mu \mu^- \bar{\nu}_\mu \mu^+ \mu^-$
ZZZ	$ZZZ \rightarrow \mu^+ \mu^- \mu^+ \mu^- l^+ l^-$
$W^+ ZZ$	$W^+ ZZ \rightarrow \mu^+ \nu_\mu \mu^+ \mu^- l^+ l^-$
tZW^+	$tZW^+ \rightarrow W^+ b \mu^+ \mu^- \mu^+ \nu_\mu \rightarrow \mu^+ \nu_\mu b \mu^+ \mu^- \mu^+ \nu_\mu$
ZZ	$ZZ \rightarrow \mu^+ \mu^- \mu^+ \mu^-$
$t\bar{t}H$	$t\bar{t}H \rightarrow W^+ b W^- \bar{b} W^+ W^- \rightarrow \mu^+ \nu_\mu b \mu^- \bar{\nu}_\mu \bar{b} \mu^+ \nu_\mu \mu^- \bar{\nu}_\mu$

Event selection

In order to detect signal events and reject background, the following selections are applied.

- The events must contain two muons with the same sign.
- Transverse moment $p_t > 25$ GeV for the highest p_t muon and $p_t > 15$ GeV for the lowest p_t muon.
- A forward jet with $p_t > 40$ GeV and $|\eta| > 2.4$
- One or more b-tagged jets with $|\eta| < 2.4$

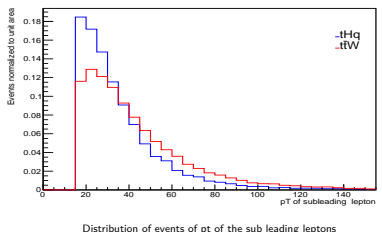
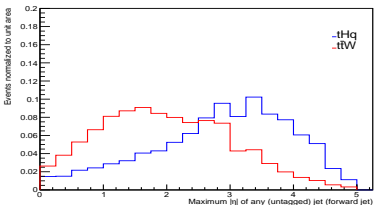
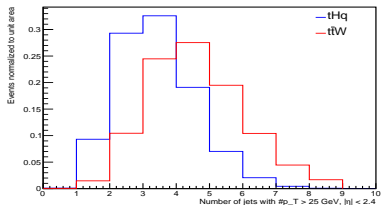
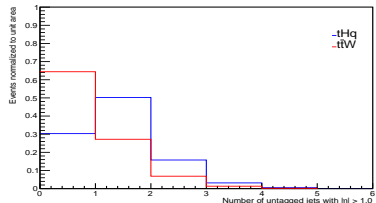
BDT

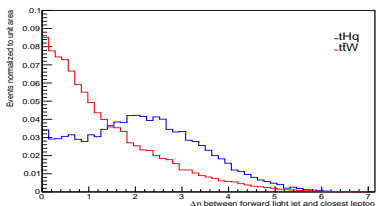
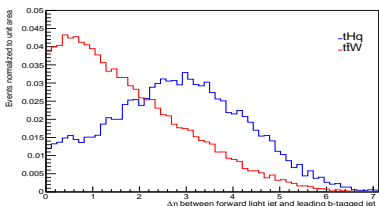
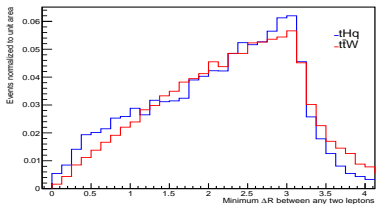
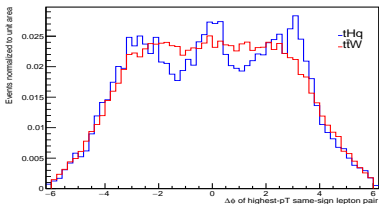
A decision tree takes a set of input features and splits input data recursively based on those features. Boosting is a method of combining many weak learners (trees) into a strong classifier. The features can be a mix of categorical and continuous data.

BDT Variables

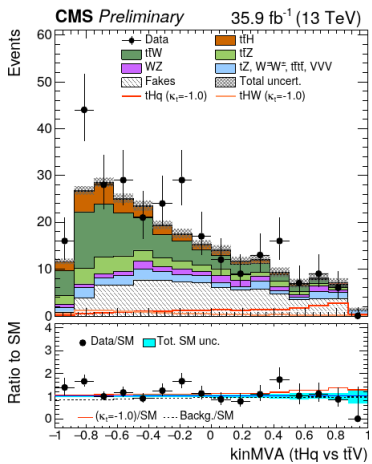
- Trailing lepton p_t
- Total charge of tight leptons
- $\min \Delta R$ (lepton pairs)
- $\Delta\phi$ between highest p_t lepton pair
- Number of jets with $|\eta| < 2.4$
- Number of non b-tagged jets with $|\eta| > 1.0$
- Maximum $|\eta|$ for jets
- $\Delta\eta$ (most forward light jet, closest lepton)
- $\Delta\eta$ (most forward light jet, hardest loosely b-tagged jet)
- $\Delta\eta$ (most forward light jet, 2nd hardest loosely b-tagged jet)



Distribution of events of p_T of the sub leading leptonsDistribution of selected events as a function of the jet with largest value of $|\eta|$ Distribution of selected events with higher pt with a $|\eta| < 2.4$ Distribution of jet events for $|\eta| > 1$

Distribution of events of $|\Delta\eta|$ between a forward jet and the closest leptonDistribution of events as function of $|\Delta\eta|$ between a forward jet and a b-tagged jetDistribution of events with a ΔR between the lepton pairs (highest and lowest pt)Distribution of events of $\Delta\phi$ between the higher pt pair of leptons

Previous results for $t\bar{t}H+tH$ production



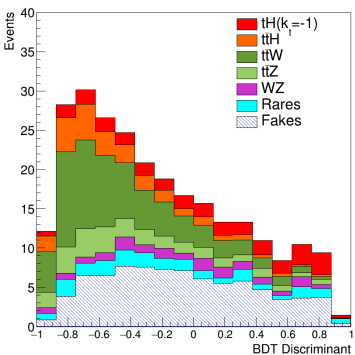
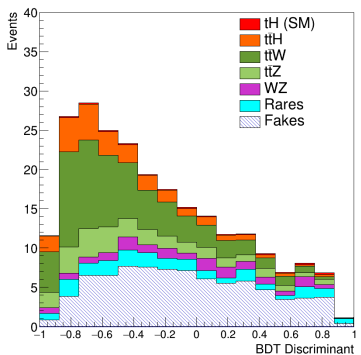
Pre-fit classifier outputs for same sign dimuon, for training against $t\bar{t}V$

Event yields for signal and backgrounds after the event selection for a integrated luminosity of 35.9 fb^{-1} . The uncertainties of yields include statistical and systematic³

Process	Number of events
$t\bar{t}W$	68 ± 10
$t\bar{t}Z$	25.9 ± 3.9
WZ	15.1 ± 7.7
Rares	20.9 ± 4.9
Fakes	80.9 ± 9.4
$t\bar{t}H$	24.2 ± 2.1
tH (SM)	2.14 ± 0.13
tH ($k_t = -1$)	26.2 ± 2.2

³ The CMS collaboration, *Search for production of a Higgs boson and a single top quark in multilepton final states in proton collisions at 13 TeV*, CMS-HIG-18-009, Phys. Rev. D 99, 092005

Distribution of events in the BDT discriminant



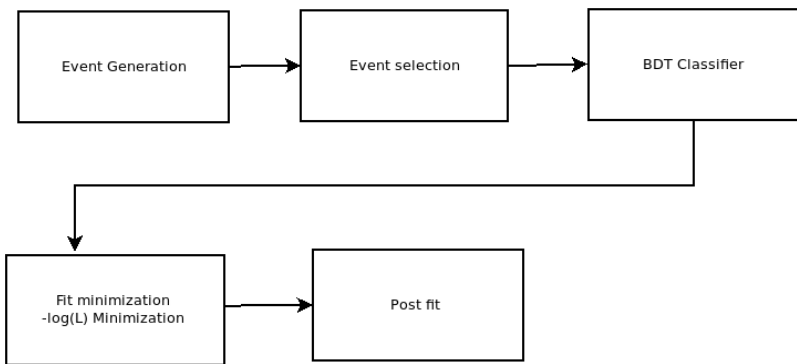
SM signal and backgrounds (Left) and $k_t = -1$ model (Right).

Systematic uncertainties

- The uncertainties on $t\bar{t}W$ and $t\bar{t}Z$ event yields are mainly due to the uncertainties of their production cross sections.
- The uncertainty on WZ background is estimated using real data events in a three lepton control region.
- In the Rare backgrounds, which are not measured, a 50% of uncertainty is assigned.
- The uncertainty on the Fakes background is estimated using real data in a control region, defined by the muon identification criteria.
- For the Higgs processes tH and ttH , the uncertainty are due to the theoretical parameters used in that simulation.



Fitting



Likelihood model

- To estimate the sensibility of the tH signal, we define an Asimov dataset, made by replacing the ensemble of simulated backgrounds and signal by a single one.
- The statistical uncertainty of the Asimov data is calculated as \sqrt{n} , with n the number of events.
- The likelihood function is the product of Poisson probabilities for all bins

$$L(\mu, \alpha) = \prod_{j=1}^N \frac{(\mu s_j + b_j)^{n_j}}{n_j!} e^{-(\mu s_j + b_j)} \prod_{k=1}^M e^{-\frac{\alpha_k^2}{2}} \quad (6)$$

where N is the total number of bins, n_j is the number of events in a bin j , s_j is the number of signal events, μ is a parameter that modifies the signal strength and b_j is the number of background events.



Likelihood model

- b_j is the sum of different background processes k

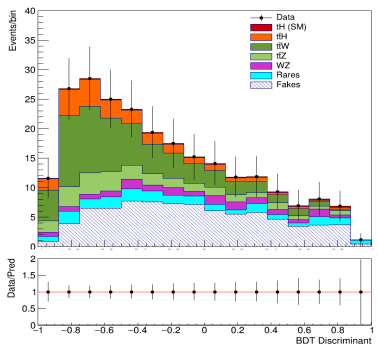
$$b_j = \sum_k^M b_j^k (1 + \alpha_k \sigma_k) \quad (7)$$

α_k is the parameter that modifies the expected background prediction and σ_k is the systematic uncertainty of the associated background. σ_k for the backgrounds are shown in the Table of yields.

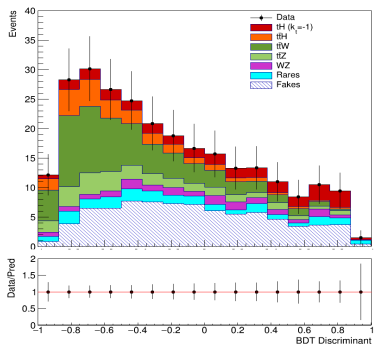
- The fit is applied by minimizing the $-\log L$ (NLL) with respect to the parameter μ and α_k . The minimization is performed by using the package ROOFIT. In the next slides, it shows the results of the model fitting using the Asimov data for the SM and the $k_t = -1$.



Results



Post-fit signal and background yields for tH process in the SM. In the box below each distribution, the ratio of the observed and event yields is shown



Post-fit signal and background yields for tH process in the $k_t = -1$. In the box below each distribution, the ratio of the observed and event yields is shown

Results

Postfit yields for the fit to the Asimov data corresponding to 35.9 fb^{-1} .
The uncertainty given is the combined statistical plus systematic.

Process	SM	$k_t = -1$
$t\bar{t}W$	68 ± 8.9	68 ± 8.9
$t\bar{t}Z$	25.9 ± 3.8	25.9 ± 3.8
WZ	15.1 ± 7.4	15.1 ± 7.4
Rares	20.8 ± 4.8	20.8 ± 4.8
Fakes	80.9 ± 9.0	80.9 ± 8.9
$t\bar{t}H$	24.2 ± 2.0	24.2 ± 2.0
tH	2.1 ± 16.5	26.2 ± 13.1

Prefit uncertainty is statistical only. Postfit uncertainty is statistical + systematic.



Results

Likelihood scan

- Due to the large background, the signal strength for the Asimov data with 35.9 fb^{-1} is consistent with zero. Therefore, we estimate an upper limit on the signal strength at 95% confidence level.
- We can define the likelihood ratio

$$\lambda(\mu, \alpha) = \frac{L(\mu, \alpha)}{L(\hat{\mu}, \hat{\alpha})} \quad (8)$$

Where $\hat{\alpha}$ and $\hat{\mu}$ are the parameters obtained in the previous section which correspond to the minimal of the NLL.

- To determine an upper limit on the strength parameter μ , we use the following statistical test

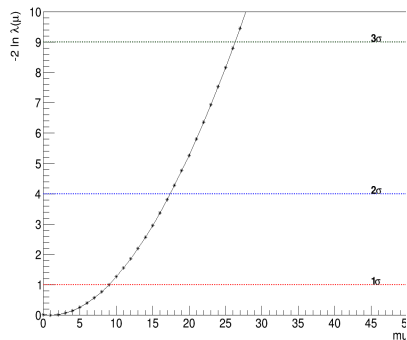
$$q(\mu, \alpha) = -2 \ln \lambda \quad (9)$$

- High values of q represent greater incompatibility between the data and the fit model. q is a random variable with a χ^2 distribution.

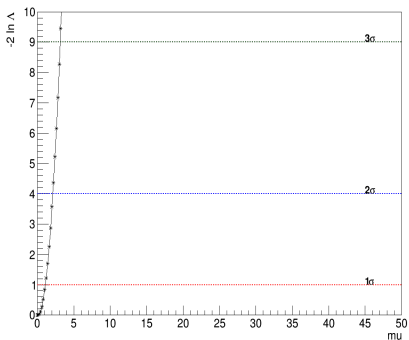


Results

Likelihood scan for an integrated luminosity of 35.9 fb^{-1}

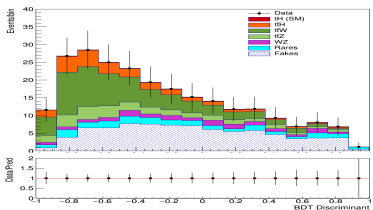


Likelihood scan for $k_t=1$ (SM)

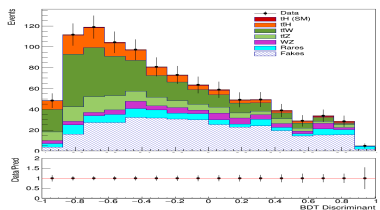


Likelihood scan for $k_t=-1$

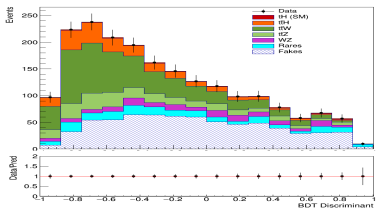
Extrapolation of luminosity for SM



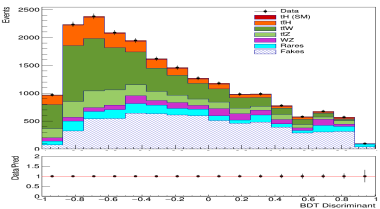
35.9 fb^{-1}



150 fb^{-1}

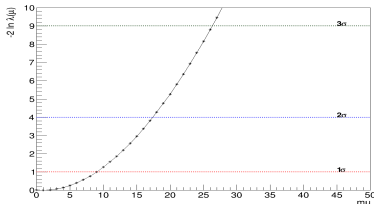


300 fb^{-1}

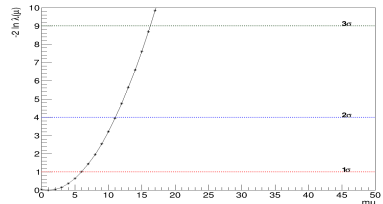


3000 fb^{-1}

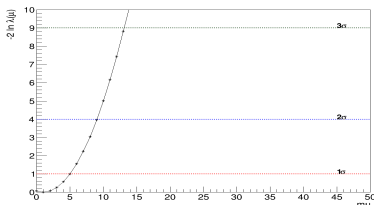
Likelihood scan for SM



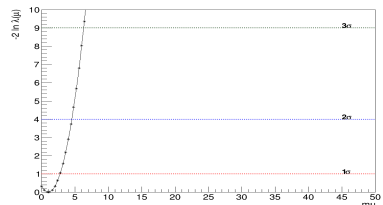
35.9 fb^{-1}



150 fb^{-1}

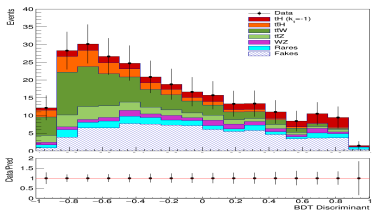


300 fb^{-1}

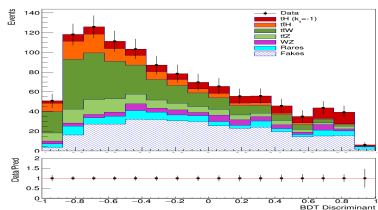


3000 fb^{-1}

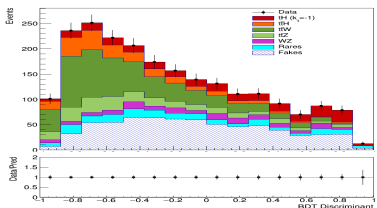
Extrapolation of luminosity for $k_t = -1$



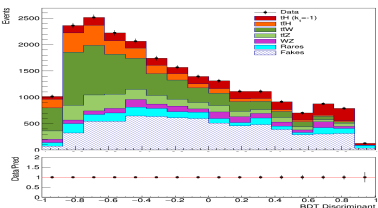
35.9 fb^{-1}



150 fb^{-1}

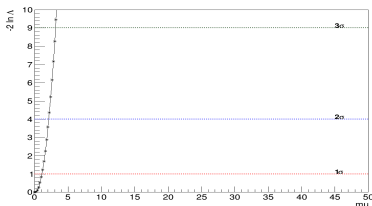


300 fb^{-1}

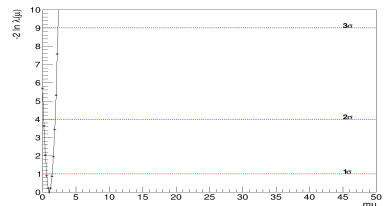


3000 fb^{-1}

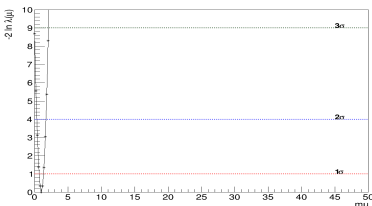
Likelihood scan for $k_t = -1$



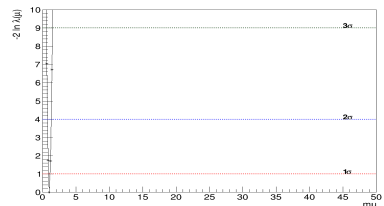
35.9 fb^{-1}



150 fb^{-1}



300 fb^{-1}



3000 fb^{-1}

Results

Upper limit

Results of μ and upper limits for Asimov extrapolations for SM and $k_t=-1$ models.

Luminosity (fb^{-1})	μ (SM)	μ (SM) upper limit	μ ($k_t=-1$)	μ ($k_t=-1$) upper limit
35.9	1.0 ± 7.7	17	1.0 ± 0.5	2.3
150	1.0 ± 6.7	11	1.0 ± 0.4	1.8
300	1.0 ± 4.3	8.7	1.0 ± 0.3	1.5
3000	1.0 ± 1.7	4.3	1.0 ± 0.1	1.1



Conclusions

- The results of the analysis for the SM case indicates that it is impossible to detect a Higgs boson using same sign dimuon channel in the tH process due to the low number of events and a huge uncertainty.
- For the SM scenario the expected uncertainty even at the largest luminosities is not enough to observe the signal and only an upper limit can be placed.
- For the $k_t = -1$, the uncertainty is low due to higher number of events for tH process and it is possible to detect a Higgs boson, but this model is purely theoretical.
- It requires a new analysis that includes more channels such as three leptons in the final state for improve the sensibility of the signal.

References

-  Gross F. *Relativistic quantum mechanics and field theory*, 1994 ,WILEY-VCH Verlag GmbH & Co. KGaA
-  Griffiths, D. *Introduction to Elementary Particles*, 2^o edition, 2008,WILEY-VCH Verlag GmbH & Co. KGaA
-  The CMS collaboration, *Search for production of a Higgs boson and a single top quark in multilepton final states in proton collisions at 13 TeV*, CMS-HIG-18-009, Phys. Rev. D 99, 092005
-  Verkerke W *Dealing with systematic uncertainties* 2014. From https://indico.cern.ch/event/287744/contributions/1641261/attachments/535763/738679/Verkerke_Statistics_3.pdf
-  ATLAS and CMS Collaborations, *Combined measurement of the Higgs boson mass in pp collisions at $\sqrt{s} = 7$ and 8 TeV with the ATLAS and CMS experiments*, Phys. Rev. Lett. 114 (2015) doi:10.1103/PhysRevLett.114.191803, arXiv:1503.07589
-  Cowan G. , Cranmer K., Gross E. , Vitells O. *Asymptotic formulae for likelihood-based tests of new physics* 2013 , arXiv:1007.1727
-  CMS collaboration *Search for tHq production in multilepton final states at 13 TeV* ,2017,CMS AN-16-378
-  CMS collaboration *High-Luminosity Large Hadron Collider (HL-LHC)*, 2017,CERN-2017-007-M

